



Magnetic Behaviour of Rare-Earth Borocarbides

Jens Jensen

Ørsted Laboratory, Niels Bohr Institute, University of Copenhagen

Collaborators:

Risø: Niels Hessel Andersen, Katrine Nørgaard Toft, Asger Abrahamsen, Des F. McMorrow (University College London), Morten Ring Eskildsen (Notre Dame).

Ørsted Laboratory: Anette Jensen, Per Hedegård.

Ames Laboratory: Paul C. Canfield, Sergey L. Bud'ko.

Hahn-Meitner Institute

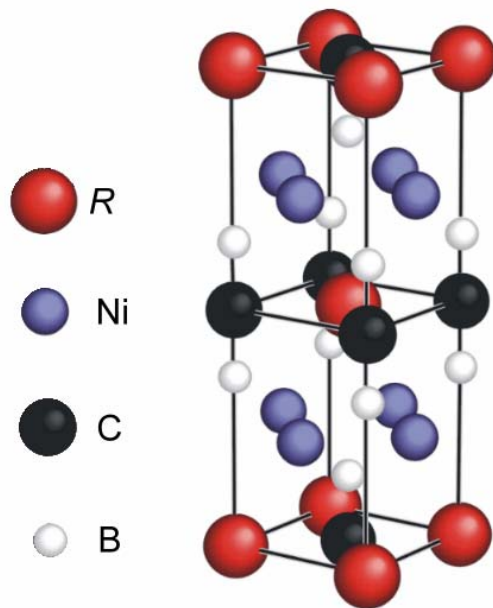
Introduction



The rare-earth borocarbides RNi_2B_2C show the coexistence of

- antiferromagnetic ordering of the rare-earth moments (below T_N)
- superconducting ordering of the conduction electrons (below T_c)

when $R = Dy, Ho, Er,$ and Tm (discovered in 1994).



Crystal structure of RNi_2B_2C

The rare-earth moments are mutually coupled via the conduction electrons (the RKKY-interaction)

→ interdependence of the magnetic and the superconducting order parameters.

The magnetic superconductors studied previously, as for example RMo_6S_8 or RRh_4B_4 , the dominating magnetic coupling is the classical dipole interaction.



Outline of the talk

1. Superconducting properties.
2. The RKKY-interaction.
3. Interdependence of magnetic and superconducting ordering.
4. Anderson-Suhl screening in $\text{TmNi}_2\text{B}_2\text{C}$.
5. $\text{TmNi}_2\text{B}_2\text{C}$ in a magnetic field.
6. Magnetic properties of $\text{ErNi}_2\text{B}_2\text{C}$.
7. The ferromagnetic component in $\text{ErNi}_2\text{B}_2\text{C}$.
8. Phase diagram of $\text{ErNi}_2\text{B}_2\text{C}$.
9. The upper-critical field in the rare-earth borocarbides.
10. Conclusion.

Superconducting properties



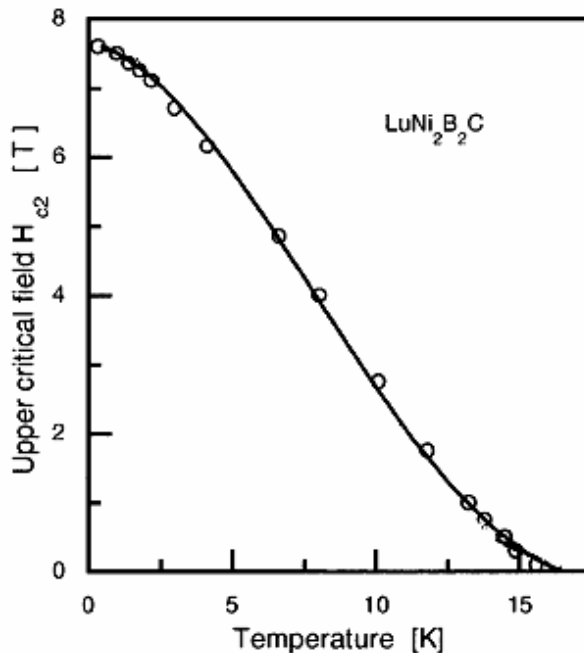
The non-magnetic “rare-earth” borocarbides $\text{LuNi}_2\text{B}_2\text{C}$ and $\text{YNi}_2\text{B}_2\text{C}$ are BCS-like type-II superconductors:

Transition temperature: $T_c \approx 15 \text{ K}$ → Superconducting energy gap: $\Delta(0) \approx 2 \text{ meV}$.

Upper critical field: $H_{c2}(0) \approx 100 \text{ kOe}$. Coherence length: $\xi(0) \approx 100 \text{ \AA}$.

Penetration depth: $\lambda(0) \approx 1000 \text{ \AA}$. Ginzburg-Landau parameter: $\kappa \approx 10$.

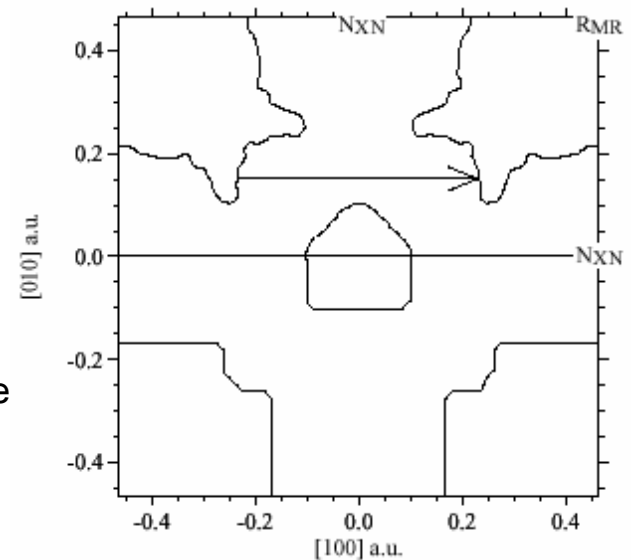
Tunneling-conductance spectra: Anisotropic behaviour of the superconducting energy gap.



Upper critical field of $\text{LuNi}_2\text{B}_2\text{C}$.

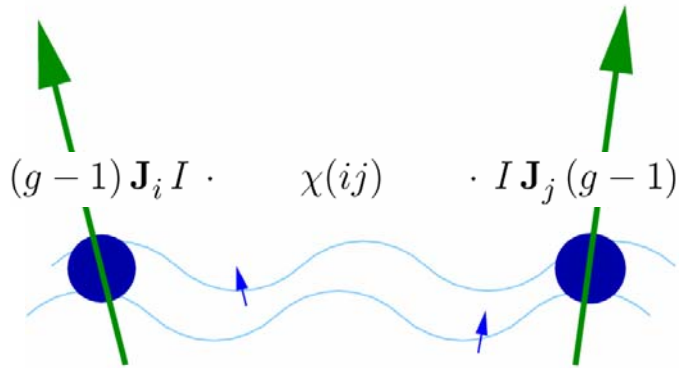
Band-structure calculations indicate nesting features at the Fermi surface around the wave vectors $Q = (0.5, 0, 0)$ and $(0, 0.5, 0)$ (in reciprocal lattice units).

This nesting is important for the phonon mediated coupling of the electrons (a softening of the transverse phonons around these wave vectors has been observed), but also for the electron mediated RKKY-exchange coupling of the rare earth moments.



The experimental (top) and calculated (bottom) Fermi surface topology of $\text{LuNi}_2\text{B}_2\text{C}$. The arrow indicates the nesting feature (after Dugdale et al.).

The RKKY interaction

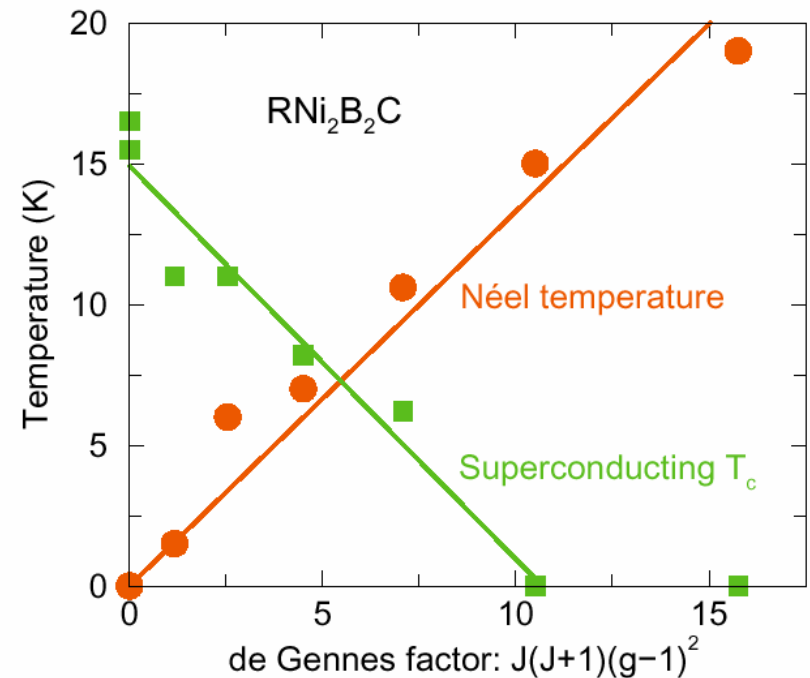


$$\mathcal{H}_{\text{RKKY}} = -\frac{1}{2} \sum_{i,j} |I|^2 (g-1)^2 \chi(i,j) \mathbf{J}_i \cdot \mathbf{J}_j$$

$$\chi(\mathbf{q}) = \frac{1}{2N} \sum_{\mathbf{k}} \frac{f(\epsilon_{\mathbf{k}}) - f(\epsilon_{\mathbf{k}-\mathbf{q}})}{\epsilon_{\mathbf{k}-\mathbf{q}} - \epsilon_{\mathbf{k}}}$$

The coupling strength, when comparing the different rare-earth borocarbides, should scale with the “de Gennes factor”:

$$G = J(J+1)(g-1)^2$$



Magnetic and superconducting transition temperatures versus the de Gennes factor.

Interdependence of magnetic and superconducting ordering



Order parameters:

Superconducting (BCS) ordering, bound state of Cooper pairs: $\Delta = \frac{g}{N} \sum_{\mathbf{k}} \langle c_{-\mathbf{k}\downarrow} c_{\mathbf{k}\uparrow} \rangle$

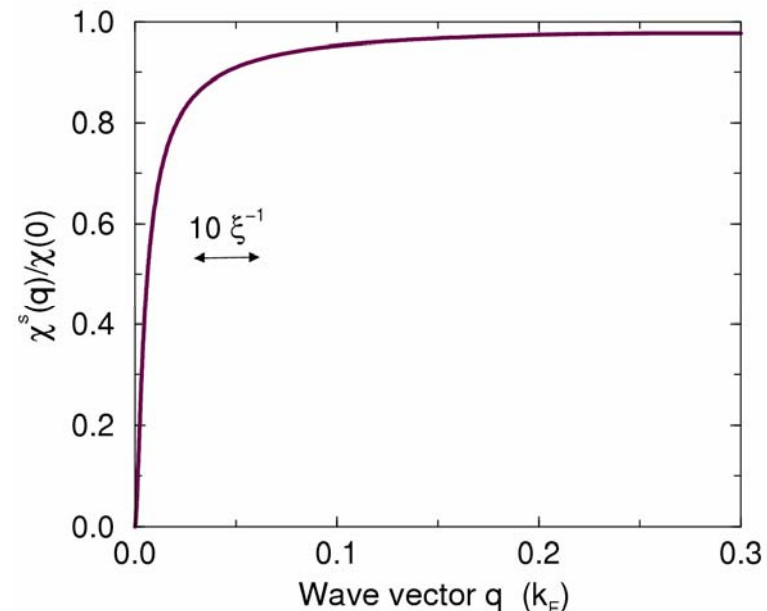
Magnetic ordering: $\langle J_z(i) \rangle = M_Q \cos(\mathbf{R}_i \cdot \mathbf{Q} + \phi)$

The Cooper pairs are affected by:

1. Magnetic “impurity” scattering [“impurity” = thermal fluctuations].
2. Magnetic “superzone energy gaps” at the Fermi surface proportional to M_Q .
3. A uniform magnetization M_0 adds to \mathbf{B} , (weak effect), but it may destroy superconductivity if the corresponding “exchange field” $\mu_B H_{\text{RKKY}} = \frac{1}{2} I(g-1) \langle J_z \rangle \geq \Delta$

The magnetic ordering is affected by changes in the electronic susceptibility:

The Anderson-Suhl (1959) screening of the uniform component (at $T = 0$):



Anderson Suhl screening in $\text{TmNi}_2\text{B}_2\text{C}$



Magnetic ordering: $\langle J_z(i) \rangle = M_Q \cos(\mathbf{R}_i \cdot \mathbf{Q} + \phi)$ $T_N = 1.5$ K, $z \parallel c$ -axis, $\mathbf{Q} = (0.09, 0.09, 0)$.
(The magnetic structure is “squared up” well below the Néel temperature).

When applying a field along the c -axis, M_Q is reduced and the antiferromagnetic phase disappears at the critical field H_N . Neutron diffraction measurements at 0.1 K shows that $H_N \approx H_{c2} = 10$ kOe.

The critical condition is:

$$[\mathcal{J}(\mathbf{Q}) - \mathcal{J}(\mathbf{0})] \langle J_z(\mathbf{0}) \rangle = g\mu_B H_N$$

where

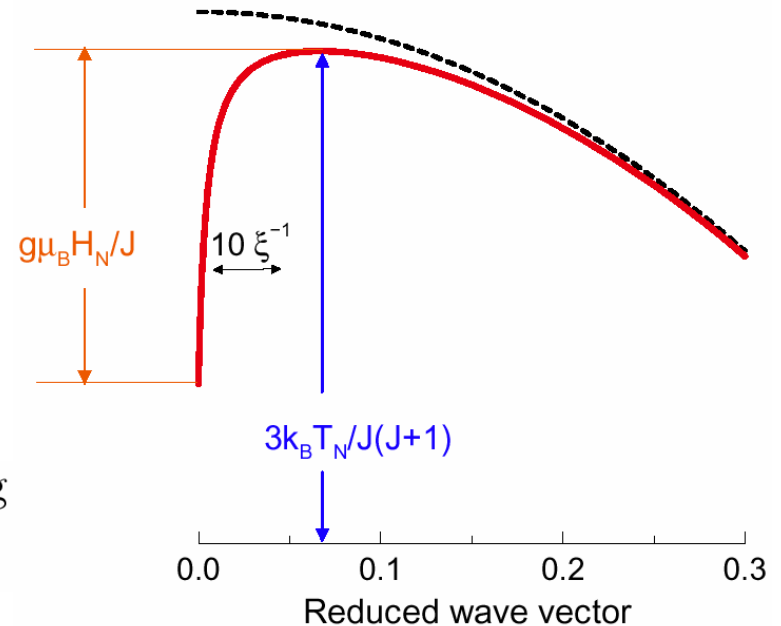
$$\mathcal{J}(\mathbf{q}) = (g - 1)^2 |I|^2 [\chi(\mathbf{q}) - \langle \chi(\mathbf{k}) \rangle]$$

$$\mathcal{J}(\mathbf{Q}) = 1/\chi_J(T_N) \approx 3k_B T_N / J(J + 1)$$

A detailed analysis shows that

$$\mathcal{J}(\mathbf{0}) \approx 0 \Rightarrow \text{estimate of } |I| \text{ indicating}$$

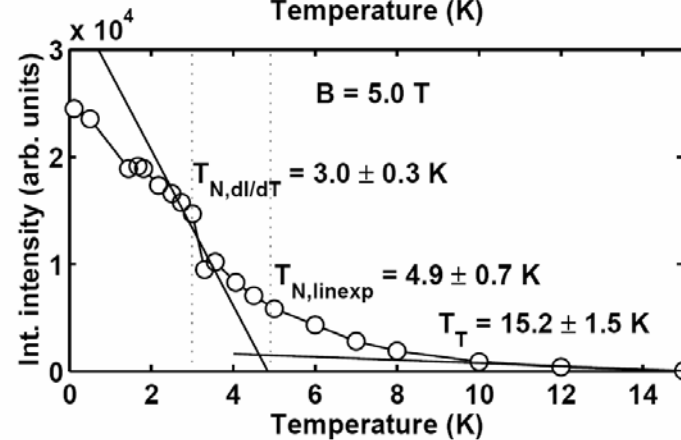
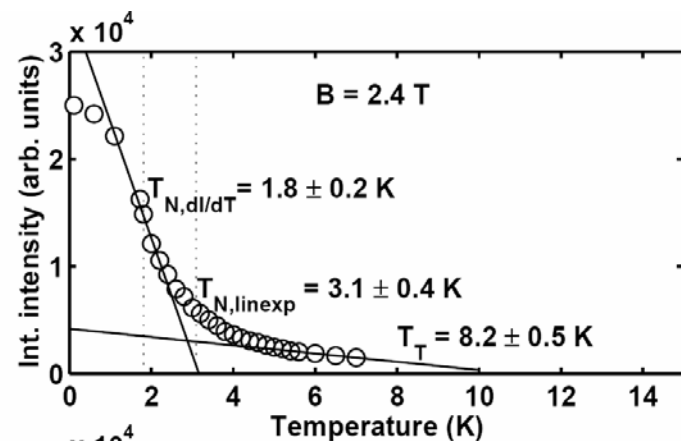
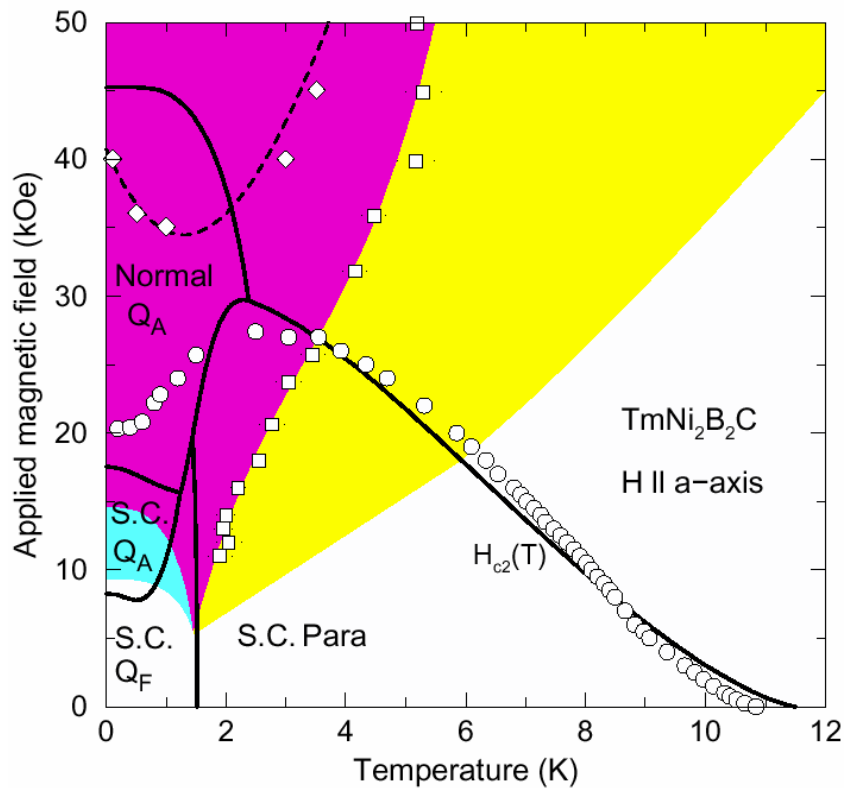
$$g\mu_B H_{\text{RKKY}} \approx \Delta \quad \text{when} \quad H \approx \frac{1}{2} H_{c2}$$



TmNi₂B₂C in a magnetic field



Field along [100]:



Nesting wave vector: $\mathbf{Q}_A = (0.48, 0, 0) \parallel \mathbf{H}$.

Quadrupolar ordering induced by a lattice distortion at \mathbf{Q}_A : $\langle O_2^1(i) \rangle = \langle J_x J_z \rangle \cos(\mathbf{Q}_A \cdot \mathbf{R}_i + \phi)$

Field along [100], the x axis, implies: $\langle J_x(i) \rangle = M_0 \Rightarrow \langle O_2^1(i) \rangle \approx \langle J_x(i) \rangle \langle J_z(i) \rangle = M_0 \langle J_z(i) \rangle$

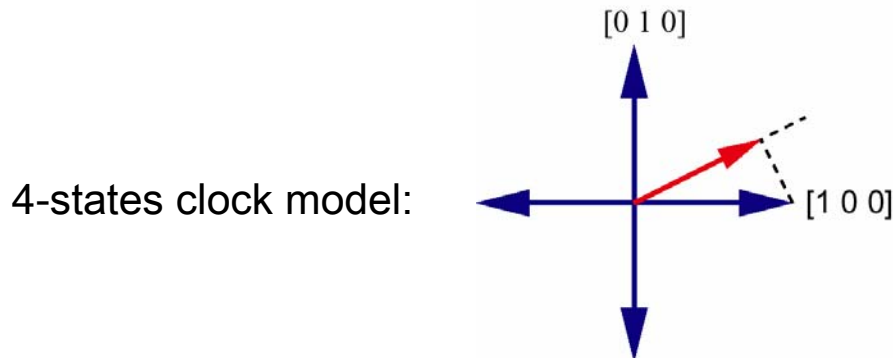
Magnetic properties of $\text{ErNi}_2\text{B}_2\text{C}$



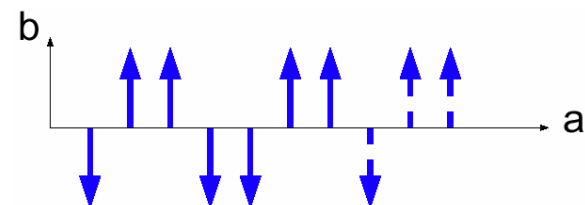
Magnetic ordering: $\langle J_z(i) \rangle = M_Q \cos(\mathbf{R}_i \cdot \mathbf{Q} + \phi)$ $T_N = 6.0 \text{ K}$, $z \parallel b$ -axis, $\mathbf{Q} = (0.554, 0, 0)$.
 The magnetic structure is “squared up” below $\sim 4 \text{ K}$ (commensurable lock-in effects),
 and $\mathbf{Q} = (0.549, 0, 0)$ below 2 K (Lynn et al.). Ferromagnetic component below
 $T_{\text{Curie}} \approx 2.3 \text{ K}$ of $\sim 0.3 \mu_B/\text{Er}$ (Choi et al.).

Orthorhombic distortion (Detlefs et al.).

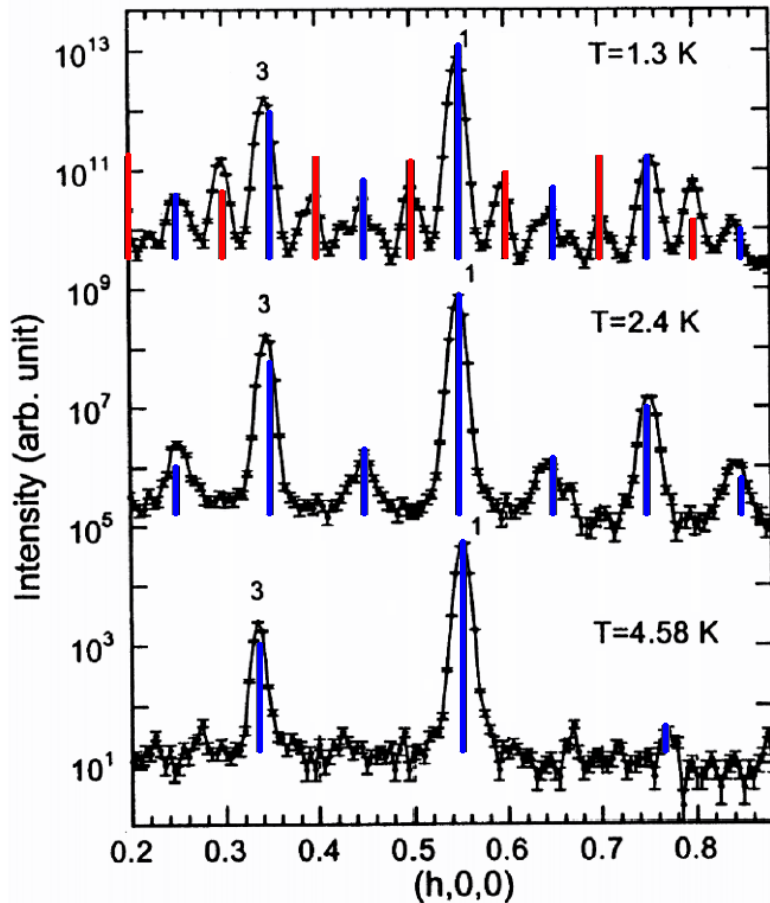
Strong crystal-field anisotropy (inelastic powder diffraction and susceptibility measurements, Gasser et al.):



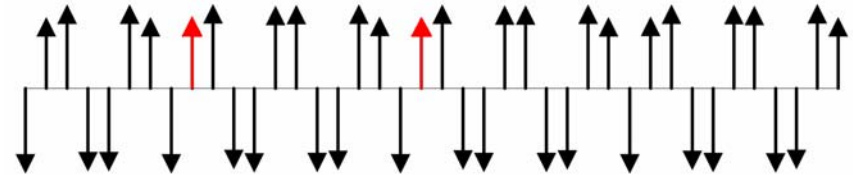
Commensurable structures:
 $\mathbf{Q} = (4/7, 0, 0)$, ferromagnetic bc layers:



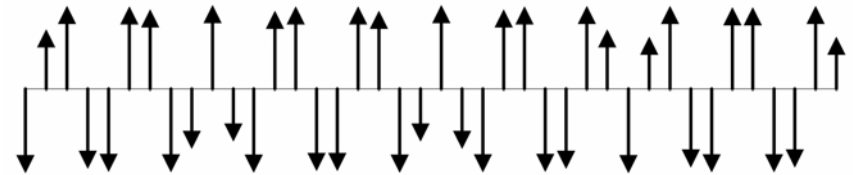
The ferromagnetic component in $\text{ErNi}_2\text{B}_2\text{C}$



Transition between two commensurate structures, both with a period of 40 bc -layers, $Q = (0.55, 0, 0)$, at $T_{\text{Curie}} = 2.3$ K:



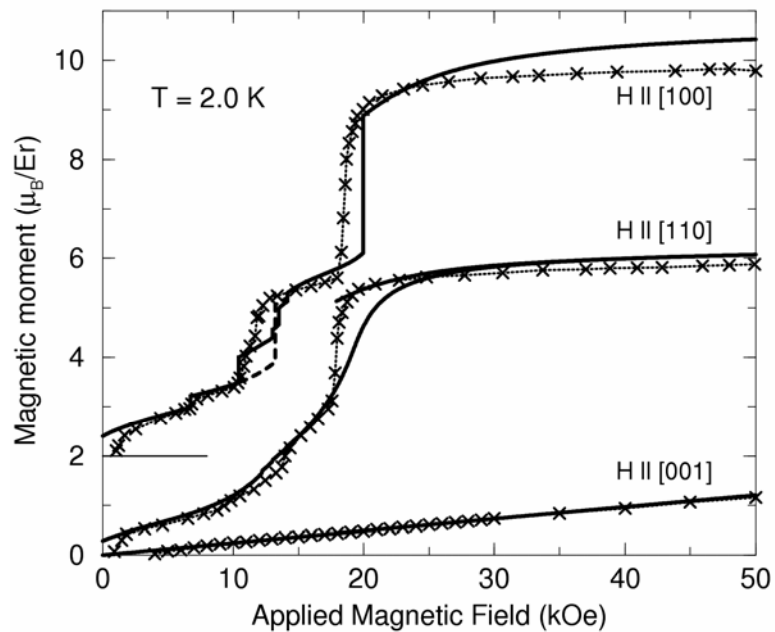
The $d(3p)d(5p)d(5p)d(5p)$ -structure below T_{Curie} (at 1.3 K).
The net moment per Er ion is approx. $8\mu_B$ times $4/40$.



The $d(4p)u(5p)u(4p)d(5p)$ -structure above T_{Curie} (at 2.4 K).
The net moment is zero.

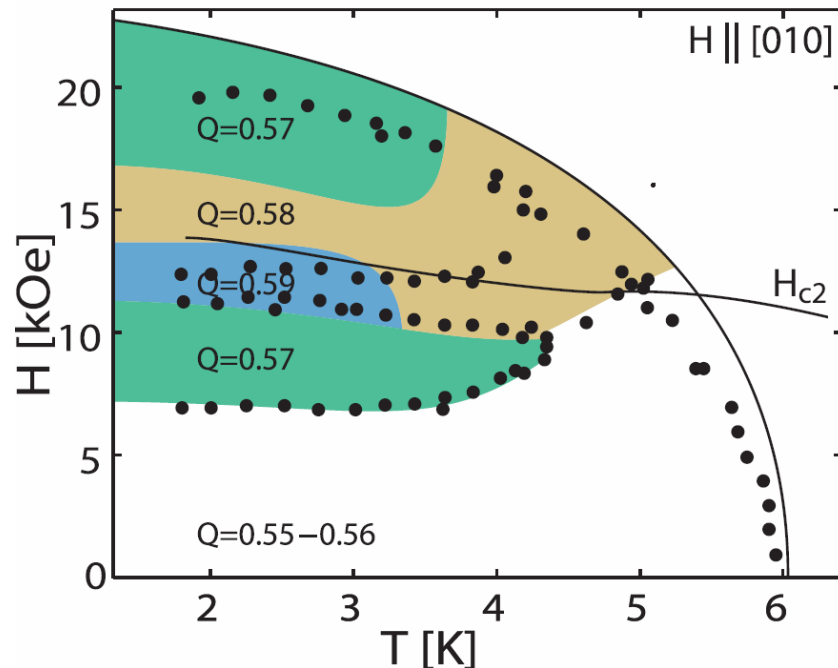
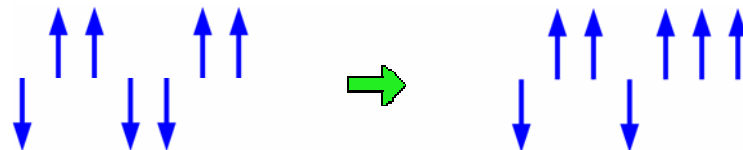
Scans along $[h,0,0]$ measured with unpolarized neutrons by Choi et al.
The data have been offset for clarity. The blue and red lines (corresponding to odd and even harmonics, respectively) are the calculated results.

Phase diagram of $\text{ErNi}_2\text{B}_2\text{C}$



The magnetization curves at 2 K. The crosses connected by dashed lines show the experimental results of Canfield et al. The remaining solid and dashed lines are the calculated results. The results in the case of $H \parallel [100]$ have been shifted upwards by 2 units.

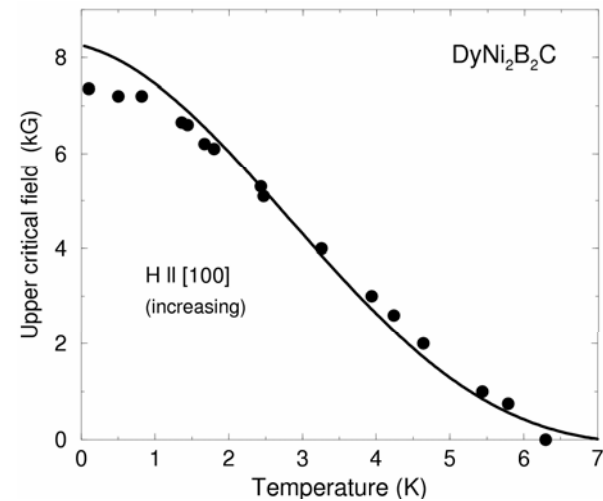
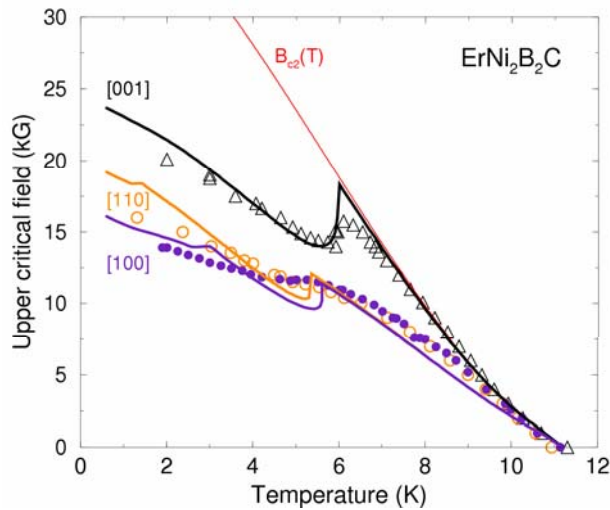
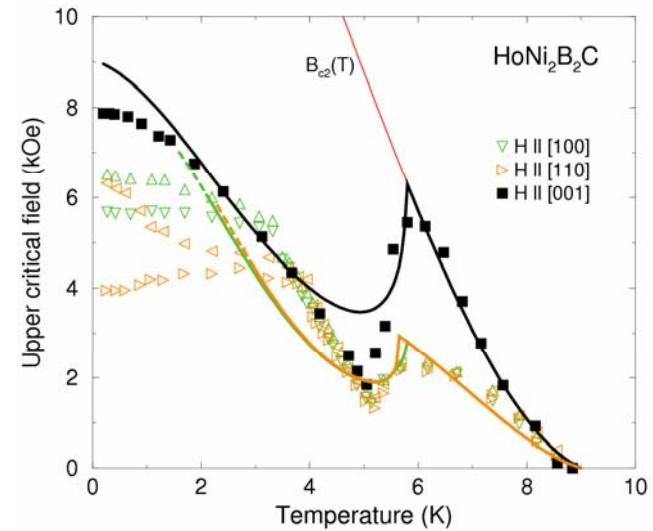
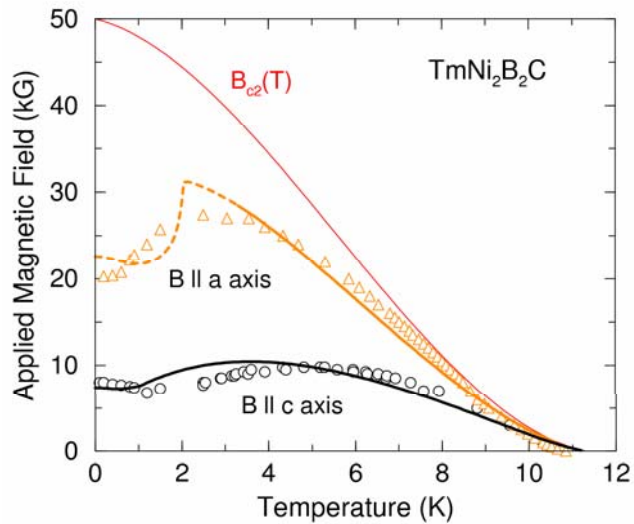
The dduu to duuu transition:



The phase diagram derived from neutron diffraction studies. The black circles denote the transitions detected in the magnetization measurements.

- Reversible behaviour of the minority domain ($Q \parallel H$) in the superconducting phase $H < H_{c2}$

The upper critical field in the rare earth borocarbides



Conclusion



1. The Anderson-Suhl screening of the electronic bulk susceptibility is important for explaining
 - the stability of the antiferromagnetic phase in $\text{TmNi}_2\text{B}_2\text{C}$.
 - the strong influence of the uniform magnetization on the upper critical field.
2. The nesting feature at the Fermi surface at $\mathbf{Q} \approx (0.5, 0, 0)$ is decisive for
 - the RKKY interaction, which, in most cases, has its maximum close to \mathbf{Q} .
 - a particular strong coupling between the conduction electrons and the phonons at this \mathbf{Q} , inducing, possibly, a quadrupolar-ordered phase in $\text{TmNi}_2\text{B}_2\text{C}$.
3. With the exception of the long wavelength antiferromagnetic phase in $\text{TmNi}_2\text{B}_2\text{C}$ and the reversible behaviour of the minority domains in $\text{ErNi}_2\text{B}_2\text{C}$, the influences of the superconducting ordering on the magnetic properties are surprisingly weak.
4. In contrast, the antiferromagnetic ordering has strong influences on the superconducting properties, i.e. the superzone gaps are efficient in reducing the available number of Cooper-pair bound states.
5. The destruction of Cooper pairs due to thermal magnetic fluctuations is probably of less significance than might have been expected. The strong magnetic anisotropy of the rare-earth ions in the superconducting compounds may be the decisive factor.